Joining and Scission in the Self-Assembly of Nanotubes from DNA Tiles

Axel Ekani-Nkodo,[1,2] Ashish Kumar,[1] and Deborah Kuchnir Fygenson[1,2,3]

[1]*Physics Department, University of California, Santa Barbara, California 93106, USA*

[2]*Materials Research Laboratory, University of California, Santa Barbara, California 93106, USA*

[3]*Biomolecular Science and Engineering Program, University of California, Santa Barbara, California 93106, USA*

(Received 5 April 2004; published 20 December 2004)

We present the first direct observations of tile-based DNA self-assembly in solution using fluorescent nanotubes composed of a single tile. The nanotubes reach tens of microns in length by end-to-end joining rather than by sequential addition of single tiles. Their exponential length distributions withstand dilution but decay via scission upon heating, with an energy barrier $E_{sc} \sim 180 k_B T$. DNA nanotubes are thus uniquely accessible equilibrium polymers that enable new approaches to optimizing DNA-based programming and understanding the biologically programmed self-assembly of protein polymers.

DOI: 10.1103/PhysRevLett.93.268301 PACS numbers: 82.35.Pq, 36.20.Cw, 61.25.Hq, 87.15.–v

The design and construction of well-defined, organized structures with nanoscale features is an important technical challenge in many scientific and engineering disciplines. Practical limitations of lithography and other top-down techniques have spurred interest in bottom-up approaches, where building blocks self-assemble into desired structures [1–5]. The scientific challenge is to understand and control the assembly process (e.g., rate, quality, geometry) based on features of the component macromolecules (e.g., structure, affinity).

DNA tiles offer a powerful, interactive approach to this challenge. Pioneered by Seeman and colleagues [6,7], DNA tiles are macromolecules made of multiple intertwined strands of synthetic oligonucleotides whose sequences are designed to place "binding sites" (i.e., single stranded regions) in definite positions and orientations relative to one another using immobile branched junctions [8]. The predictability and specificity of Watson-Crick base pairing thus enables programmable self-assembly of extended structures with nanometer resolution and tunable stability [9].

In recent years a variety of beautiful structures and clever designs have been realized using DNA tiles (see, e.g., [10–13]). Among these, self-assembling tubes offer a distinct experimental advantage as a model system in which to study the assembly process. The cylindrical architecture stiffens the tile lattice, enabling real-time observation of individual assemblies in solution via optical microscopy. The best characterized DNA tubes to date have a diameter between 7 and 20 nm and a persistence length of at least 4 μm [13].

In this Letter, we characterize the tile-based assembly dynamics of these DNA nanotubes. Their steady state length distribution is exponential, and the approach to equilibrium is dominated by joining and scission events, which can be observed directly. DNA nanotubes may therefore be classified as a novel type of "living" polymer [14]. An important consequence of this dynamic is a high density of defects in the DNA tile lattice. These results lay a foundation for testing theories of living polymerization and exploring tile designs that may lead to longer, more perfect assemblies.

We use a single DNA tile of the DAE-E type [6] designed to form a lattice with intrinsic curvature perpendicular to the long axis of the tile [13]. (See Fig. 1.) The five oligomers that compose the DAE-E tile are combined in solution [15], heated to 95 °C, cooled slowly to 25 °C, and left overnight at room temperature to reach steady state. A fluorophore covalently bound to one of the oligomers allows the length and shape of the resulting nanotubes to be measured by optical microscopy [16]. Thin (2–3 μm) samples of bare or poly(vinyl pyrrolidone) PVP coated glass [17] confine the nanotubes to the

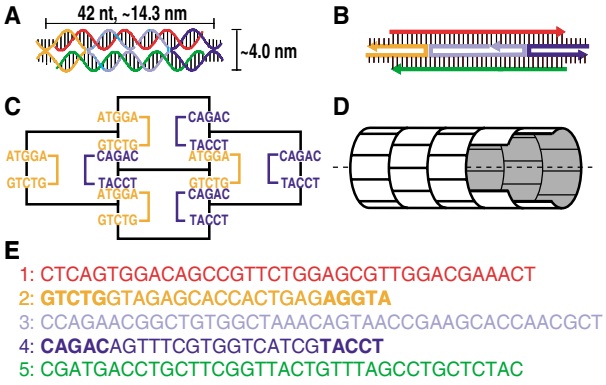

FIG. 1 (color). DNA tile used in this study. (a) Structural schematic showing the intertwining of the five DNA strands. Five unpaired bases at both ends of the rightmost (orange) and leftmost (blue) strands are sticky ends, responsible for directing tile assembly. (b) Cartoon clarifying interstrand base pairing. (c) Local arrangement of tiles into crystals with paired sticky end sequences explicit. (d) Global geometry of the intrinsically curved tile lattice that forms hollow tubes with between four and ten tiles around [13]. (e) Complete sequences of the five DNA oligonucleotides. Bases that participate in sticky ends are boldface.

focal plane of the microscope so that their lengths can be accurately measured.

Cooling in 5 °C steps of 20′ duration results in nanotubes with a median length of 5.8 μm. Cooling 3 times more slowly (5 °C/60′) results in a median length almost twice as large, 10.3 μm. Cooling at this slower rate but in smaller steps (1 °C/12′) results in a similar median, 11.3 μm. Cooling continuously at a comparable rate ($t_{1/2} \approx 7$ h) increases the median length to 15 μm. In all cases, the steady state length distribution is exponential, so the effect of the cooling rate is most noticeable in the tail of the distribution. Of 411 nanotubes measured in the 5 °C/60′ sample, only two reached 50 μm in length. Of 197 nanotubes measured in the 1 °C/12′ sample, eight were over 50 μm and the longest was almost 90 μm. Similarly, 28 out of 787 nanotubes measured in the continuous sample were over 50 μm long, but the longest were over 120 μm.

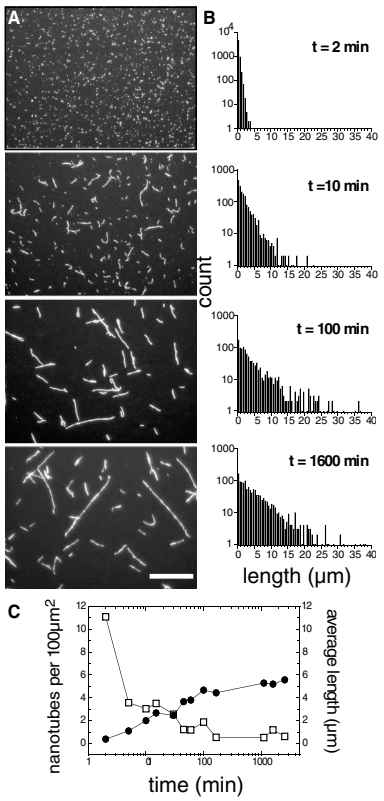

FIG. 2. Nanotube assembly from preformed tiles following a quench (45 °C → 22 °C). At various times after the quench, a small amount of solution was diluted to 40 nM and deposited on bare glass [17]. Adhesion to the glass stopped the assembly reaction and facilitated measurement of short nanotubes. (a) After 2 min, small aggregates appear. At 10 min, tubes are clearly visible. After 100 min, long tubes (> 20 μm) are present. More than a day later, tubes >50 μm can be found. Scale bar: 20 μm. (b) The distribution of nanotube lengths is exponential at all times. (c) Average length (●) increases while nanotube density (□) decreases over time. Steady state is reached after ~1000 min.

The exponential character of the length distribution suggests that these polymers pass through an "equilibrium" or living phase of assembly, wherein tiles are readily exchanged between nanotubes [14]. We find direct evidence of such an assembly mechanism by tracking the length distribution following a rapid quench into the assembly region (Fig. 2). For the first minute after quench, the sample appears empty, but within two minutes a high density of short nanotubes is seen [Fig. 2(a)]. The distribution of lengths remains exponential at all intermediate times [Fig. 2(b)], but the number of nanotubes per field of view decreases steadily as the characteristic length increases [Fig. 2(c)]. This monotonic decrease in density suggests that nucleation is essentially over by the time nanotubes are large enough to be detected (~0.5 μm) and, from then on, long tubes form while short ones disappear. Such "coarsening" or "ripening" can happen either by the loss of tiles from one tube and their addition to another or by end-to-end joining or both [18,19].

To assess the relative importance of these two assembly mechanisms, we tracked the length of several individual nanotubes over time. Even after dilution to a total tile concentration of 10 nM (1/40 of the original assembly concentration), long nanotubes (> 40 μm) were present and stable. Single tubes showed no detectable changes in length over two hours of observation. We did observe, however, several spontaneous end-to-end joining events (Fig. 3). At the low densities where single tubes can be tracked (< 40 nM), the probability for such events is necessarily rare. In a total of ~12 h of recording encompassing dozens of nanotubes, four such events were captured. In one of the four, the end of one nanotube attaches to the side of another, and the two then align to create a "single" nanotube with a ~1 μm stretch of increased brightness in the middle. Joining events are thus not restricted to occur at the ends of nanotubes.

We confirmed the importance of tube joining at higher concentrations using a method similar to that of Murphy *et al.* [20]. Two solutions of nanotubes labeled with either green or red fluorescent dye were mixed together at 400 nM, sonicated at 47 kHz for 30 s, and left at room temperature for 48 h. Subsequent imaging revealed numerous patched nanotubes, with alternating green (left) and red (right) sections (see Fig. 3). Aligned and superimposed images of patched nanotubes occasionally reveal doubly labeled regions between patches of different colors, further documenting the possibility of overlap during joining events.

In contrast to joining, no instance of the reverse event, scission, was captured in all our observation time at room temperature. Scission is an important mechanism, however, in nanotube disassembly. This is evidenced by a sharp increase in nanotube number density with increasing temperature as the length distribution shifts to lower

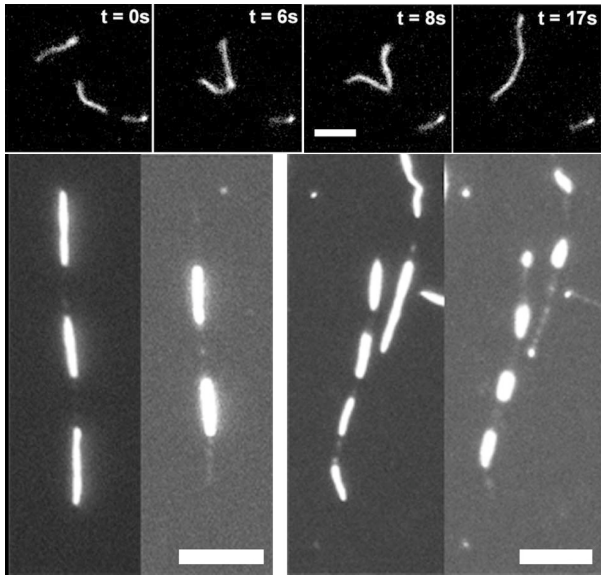

FIG. 3. Top panels: Stills from a movie in which two short nanotubes join end to end, forming a single nanotube. Bottom panels: End-to-end joining results in patched nanotubes. Tiles labeled with green and red fluorescent dye were assembled separately, mixed, sonicated briefly and left to equilibrate for 48 h. Two examples are shown in which the same field of view is imaged with both green (left) and red (right) filter sets. Scale bars: 5 μm.

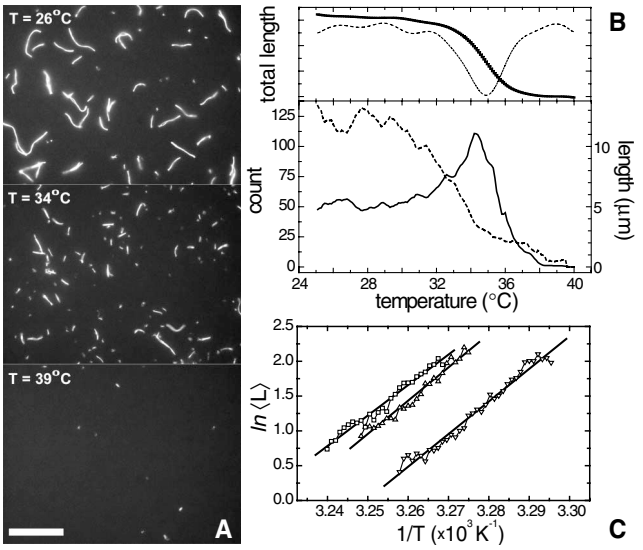

FIG. 4. Nanotubes disassemble upon heating via scission. (a) Representative fields at increasing temperature. Scale bar: 20 μm. (b) Top: Total polymer length (per field of view) exhibits a typical melting curve shape (solid line). The derivative (dashed line) peaks at $\sim$35 °C. Bottom: As the average length (dashed line) steadily decreases, the number of nanotubes per field of view (solid line) increases, peaking when $\langle L\rangle \sim 4$ μm, before decreasing to zero. (c) $\langle L\rangle$ versus $1/T$ for nanotube solutions prepared at three different cooling rates: 5 °C/5′ (∇), 5 °C/20′ ($\square$), 5 °C/60′ ($\triangle$). The slope is proportional to E_{sc}, the scission energy required to create two new ends. Linear fits to the three data sets yield an average value $E_{sc} = 110$ kcal/mol $\sim 180 k_B T$.

lengths [Figs. 4(a) and 4(b)]. The total polymer length (i.e., estimated from the product of the average length and the number of nanotubes in a field of view) has a typical melting curve shape, with an effective melting temperature, $T_m \sim 35$ °C, given by the peak in the derivative curve [Fig. 4(b)]. This temperature is within a few degrees of the melting temperature predicted for a single five base pair sticky end, once stacking interactions at both ends are taken into account [21].

The energy barrier for scission, deduced [19] from the temperature dependence of the average length, $\langle L\rangle \propto \exp(E_{sc}/2k_BT)$, is relatively high by comparison, $E_{sc} = 110$ kcal/mol $\sim 180 k_B T$ [Fig. 4(c)]. This makes sense given the greater number of bonds that must be broken to sever a tube, but should be high enough to prohibit scission altogether.

The likely explanation is that the nanotube wall is riddled with defects from which tiles can easily dissociate. The existence of free sticky ends within the tile lattice is implied from our observation of joining events involving sites in the middle of a tube. Furthermore, static domains of different fluorescence intensity are common along individual nanotubes [see, e.g., Fig. 2(a), bottom panel]. Because of the well-defined stoichiometry of labeling (one dye molecule covalently bound to each tile) and the small tile size (a diffraction limited tube segment contains >50 tiles) [Fig. 1(a)], fluorescence intensity should be a good indicator of relative tile density.

We suggest that a primary source of defects is imperfect joining, in which nanotubes with, for example, jagged ends or different diameters attach without satisfying all their sticky ends. Fluorescence intensity domains would then be a good indicator for testing assembly protocols and tile designs that would minimize joining in assembly. In this light, it is interesting to compare DNA nanotubes to their biological analogs, self-assembled tubes of protein, called microtubules. Microtubules have a high barrier to nucleation [22], rarely disassemble via scission [23], and contain few lattice defects [24]. Perhaps the comparative shortcomings of DNA nanotubes are due to less stringent geometric constraints on subunit interactions. Lattice integrity may be optimized by reducing nanotube density during assembly (moving to lower tile concentrations or even more gradual cooling rates), or by altering tile design, for example, to include longer (stronger, more specific) sticky ends. One might also test for correlation between intensity, thermal stability, and bending stiffness.

DNA tiles are more stable than proteins, and their nanotube assemblies are more easily handled and visualized than synthetic polymers. They are therefore promising candidates for the testing of theories regarding equilibrium polymers. Experimental determination of

molecular weight distributions for such polymers is a difficult task [25]. The length distributions presented here directly verify predictions of an exponential distribution [19,26]. Experiments to test other predictions (e.g., how average polymer length scales with concentration) are in progress.

We have capitalized on the unique accessibility of DNA nanotubes for optical microscopy to study the mechanism of tile-based self-assembly. These studies lay a foundation for gaining control over the assembly mechanism and eventually for being able to tune attributes of potential practical importance, such as thermal stability, bending stiffness, and length distribution, via sequence design.

DNA nanotubes are also an interesting platform for biomimicry. In the natural nanotechnology of cells, microtubules serve as structural supports and pathways for transport. Their tubular construction is important for its stiffness, but also for its interior compartment and the possibility it affords for coordinating cooperative interactions [27]. DNA nanotubes present an opportunity for rational design aimed at *de novo* reproduction of microtubule based phenomena such as active transport and dynamic instability. The recapitulation of such phenomena with completely abiological structures would be the ultimate test of our understanding of the principles underlying biological macromolecular design.

We thank P.W. K. Rothemund and E. Winfree for introducing us to DNA nanotubes, for the generous gift of DNA strands, and for many insightful conversations. We thank N. Papadakis for technical assistance in the early stages of the project and D. Pine for directing our attention to the equilibrium polymer literature. This work was supported in part by the National Science Foundation through the MRSEC Program under Grant No. DMR00-80034, by the Alfred P. Sloan Foundation (D. K. F.), and by the Institute for Collaborative Biotechnologies through Grant No. DAAD19-03-D-0004 from the U.S. Army Research Office.

[1] N. C. Seeman and A. M. Belcher, Proc. Natl. Acad. Sci. U.S.A. **99**, 6451 (2002).
[2] C. A. Mirkin *et al.*, Nature (London) **382**, 607 (1996).
[3] A. P. Alivisatos *et al.*, Nature (London) **382**, 609 (1996).
[4] E. Braun *et al.*, Nature (London) **391**, 775 (1998).
[5] C. J. Loweth *et al.*, Angew. Chem., Int. Ed. Engl. **38**, 1808 (1999).
[6] T. J. Fu and N. C. Seeman, Biochemistry **32**, 3211 (1993).
[7] X. Li, X. Yang, J. Qi, and N. C. Seeman, J. Am. Chem. Soc. **118**, 6131 (1996).
[8] N. C. Seeman, J. Theor. Biol. **99**, 237 (1982).
[9] N. C. Seeman, Nature (London) **421**, 427 (2003).
[10] E. Winfree *et al.*, Nature (London) **394**, 539 (1998).
[11] T. H. LaBean *et al.*, J. Am. Chem. Soc. **122**, 1848 (2000).
[12] H. Yan *et al.*, Science **301**, 1882 (2003).
[13] P.W. K. Rothemund *et al.*, J. Am. Chem. Soc. **126**, 16344 (2004).
[14] S. Greer, Annu. Rev. Phys. Chem. **53**, 173 (2002).
[15] HPLC purified DNA oligomers were purchased from Integrated DNA Technologies (Coralville, IA). Each oligomer was brought to a stock concentration of 10 μM in pure water, as determined by UV absorbance, and stored at 20 °C. The five oligomer stock solutions were combined and diluted to a final concentration of 400 nM each in buffer whose final concentration was 40 mM tris-acetate, 1 mM ethylene diamine tetra-acetic acid, and 12.5 mM Mg-acetate at a *p*H of 8.3.
[16] The fluorophore, either fluorescein (FAM) or carboxytetramethylrhodamine (TAMRA), was located at the 3′ end of either the 1, 3, or 5 strand [Fig. 1(e)], with no apparent position dependent effect. An oxygen scavenging system enables extended observation with minimal photobleaching. Samples were prepared for imaging, by adding 1 μL of a 10× oxygen scavenging mix (45 mg/ml glucose, 2.0 mg/ml glucose oxidase, 0.35 mg/ml catalase, 5% β-mercaptoethanol) to 9 μL of nanotube solution. Then 1.5 to 2.5 μL of the resulting solution was deposited onto a slide, covered with a cover slip, and sealed with 5-min epoxy.
[17] The high concentration of Mg^{++} in the buffer solution mediates the strong adsorption of DNA on bare glass. The deposition is not homogeneous across the sample, however. In some regions, immobilized nanotubes appear locally aligned, presumably due to flows generated during sample preparation. In other regions, an excess of short tubes suggests that the resulting shear can be strong enough to break tubes, potentially biasing the distribution toward shorter lengths. PVP coating prevents nanotubes from sticking to the glass, ensuring that measurements are not confounded by breaking or bending induced by the strong surface interactions. The coating procedure was adapted from K. Srinivasan, G. Pohl, and N. Avdalovic, [Anal. Chem. **69**, 2798 (1997)]. Before coating, slides and cover slips were cleaned by sonication in soapy water (Micro, Cole Parmer) at 60 °C for 30′, rinsed copiously in deionized water and stored in ethanol.
[18] F. Oosawa and S. Asakura, *Thermodynamics of the Polymerization of Protein* (Academic Press, New York, 1975).
[19] M. Cates and S. Candau, J. Phys. Condens. Matter **2**, 6869 (1990).
[20] D. B. Murphy *et al.*, J. Cell Biol. **106**, 1947 (1988); S.W. Rothwell *et al.*, J. Cell Biol. **102**, 619 (1986).
[21] As determined from the *m*-fold server of M. Zuker, Nucleic Acids Res. **31**, 3406 (2003), for 400 nM concentration with 10 mM Na^{+}, 12.5 mM Mg^{++}. Bases were added at each end to take into account stacking interactions, but were not allowed to pair.
[22] D. K. Fygenson *et al.*, Phys. Rev. E **51**, 5058 (1995).
[23] R. B. Rye *et al.*, Cell Motil. Cytoskeleton **21**, 171 (1992).
[24] D. Chrétien and R. H. Wade, Biol. Cell **71**, 161 (1991).
[25] S. Sarkar Das *et al.*, J. Chem. Phys. **111**, 9406 (1999).
[26] P. van der Schoot, Europhys. Lett. **39**, 25 (1997).
[27] J. L. Ross *et al.*, Proc. Nat. Acad. Sci. U.S.A. **101**, 12 910 (2004).